15. S. A. Schulz, L. O'Faolain, D. M. Beggs, T. P. White, A. Melloni, and T. F. Krauss, "Dispersion engineered slow light in photonic crystals: a comparison," J. Opt. **12**, 104004 (2010).
16. L. O'Faolain, S. A. Schulz, D. M. Beggs, T. P. White, M. Spasenović, L. Kuipers, F. Morichetti, A. Melloni, S. Mazoyer, J. P. Hugonin, P. Lalanne, and T. F. Krauss, "Loss engineered slow light waveguides," Opt. Express **18**, 27627–27638 (2010).
17. J. Li, T. P. White, L. O'Faolain, A. Gomez-Iglesias, and T. F. Krauss, "Systematic design of flat band slow light in photonic crystal waveguides," Opt. Express **16**, 6227–6232 (2008).
18. W. Jiang, K. Okamoto, F. M. Soares, F. Olsson, S. Lourdudoss, and S. J. Yoo, "5 GHz channel spacing InP-based 32-channel arrayed-waveguide grating," in "Optical Fiber Communication Conference," (Optical Society of America, 2009), p. OWO2.
19. F. Wang, J. S. Jensen, J. Mørk, and O. Sigmund, "Systematic design of loss-engineered slow-light waveguides," J. Opt. Soc. Am. A **29**, 2657–2666 (2012).

1. Introduction

"Slow light" methods [1], which refer to a broad category of science and technology that aims at controlling the group index of optical materials, have recently been studied extensively [2–4] for applications such as optical buffers, interferometry, laser radar, nonlinear photonics, etc. Specifically, it has recently been shown that slow light methods can greatly enhance the performance of spectroscopic interferometers of various geometries [5–10]. Moreover, slow-light techniques can greatly reduce the size of a spectroscopic interferometer while maintaining high spectral resolution, and they therefore show promise for the development of miniaturized on-chip spectrometers. In photonic integrated circuits, arrayed waveguide gratings (AWGs) [11] are a common spectrometer geometry that is widely used in telecommunications and other areas. It has recently been shown that the spectral performance of an AWG can be greatly enhanced by replacing a normal waveguide array with the slow-light waveguide array [12, 13].

In ideal situations where the slow-light waveguides are lossless, the enhancement factor of the spectral resolution of a slow-light AWG is proportional to the group index of the waveguides [12, 13]. However, practical slow-light technologies, such as photonic crystal (PhC) line-defect waveguides [14–16], often possess associated loss, and it is unclear what the role of loss is in degrading the spectral performance of slow-light AWGs. In this paper, we derive analytically an expression for the spectral performance of a slow-light AWG in the presence of loss. We show that the fundamental limiting spectral resolution of a slow-light AWG scales as the loss–group-index ratio of the waveguides. We further show that by using currently available PhC slow-light technologies, one can achieve spectral resolutions comparable to or better than those achieved in conventional AWGs while significantly reducing the footprint of the device.

An AWG is typically comprised of three parts as shown in Fig. 1. The input signal field first passes through a free propagation region (FPR) where its beam size expands due to diffraction. The expanded field is then coupled into an array of waveguides, which are designed such that the length of neighboring waveguides differs by a fixed amount $\Delta l = m\lambda_0/n_{\text{eff}}$, where λ_0 is the designed central (vacuum) wavelength of the device, n_{eff} is the mode index of the waveguides, and m is the diffraction order of the waveguide grating. The outputs of these waveguides are spaced evenly with a spatial period of Λ along the input to a second FPR. The exiting fields from the waveguide array interfere and different wavelengths focus at different transverse locations of the other side of the second FPR, where they can be further separated by coupling into different output waveguides. A slow-light AWG has the same geometry as a conventional AWG, except that the neighboring waveguides differ by a fixed length Δl of slow-light waveguides whose mode group index $n_g \equiv n_{\text{eff}} + \omega dn_{\text{eff}}/d\omega$ can be much larger than its mode index n_{eff}.

#182813 - $15.00 USD Received 7 Jan 2013; revised 8 Mar 2013; accepted 15 Mar 2013; published 22 Mar 2013

2. Performance of a slow-light AWG spectrometer

The diffraction equation of an AWG is given by [11],

$$n_{\text{eff}}\Delta l + n_{\text{s}}\Lambda(\sin\theta_{\text{inc}} + \sin\theta_{\text{d}}) = m\lambda, \tag{1}$$

where n_{eff} and n_{s} are the effective mode indices for the waveguides and the slab FPR, respectively. Note that we here assume that the neighboring waveguides in the waveguide array are differed by a fixed length of only one type of waveguide as shown in the purple triangle region in Fig. 1, whose mode index is denoted by n_{eff}. The actual waveguide may contain sections of other types of waveguide, e.g., the conventional waveguides outside the purple region as plotted in Fig. 1. However, we assume here that the conventional waveguide sections are of the same length through out the waveguide array, and therefore the length and mode index of these conventional waveguides do not appear in the AWG diffraction equation of Eq. (1). By taking the derivative of Eq. (1) with respect to ω, one obtains its angular dispersion as follows [13],

$$\frac{d\theta_{\text{d}}}{d\omega} \approx \frac{n_g\Delta l}{n_{\text{s}}\omega\Lambda\cos\theta_{\text{d}}} = \frac{2\pi c n_g m}{n_{\text{s}}n_{\text{eff}}\omega^2\Lambda\cos\theta_{\text{d}}}. \tag{2}$$

Note that the approximated expression is obtained by assuming $dn_{\text{s}}/d\omega = 0$, and that the second expression is obtained by using the relation $\Delta l = m\lambda_0/n_{\text{eff}}$.

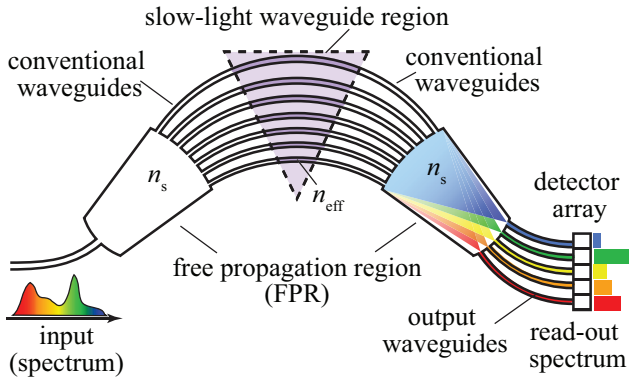

Fig. 1. Schematic diagram of a slow-light arrayed-waveguide-grating spectrometer.

At the center frequency, the output fields from different waveguides of the array are in phase. Thus, the total field distribution at the exit plane of the waveguide array, i.e., the input to the second FPR, can be mathematically approximated by [see Fig. 2(a)]

$$E(x) \propto \left[\text{comb}\left(\frac{x}{\Lambda}\right)\text{Rect}\left(\frac{x}{N\Lambda}\right)A(x)\right] * E_{\text{wg}}(x), \tag{3}$$

where N is the total number of waveguides in the array, $A(x)$ is the envelope function of the peak amplitude of the field at the exit of each waveguide, $*$ denotes convolution, and $E_{\text{wg}}(x) \approx \exp(-0.5x^2/\sigma^2)$ is the spatial mode profile of each waveguide, and where σ denotes the $1/e$ half width of the waveguide mode [see Fig. 2(a)].

When the loss of the waveguides is negligible, the envelope function $A(x)$ is equal to the envelope of the field at the entrance of the waveguide array, which is the mode profile of the input waveguide broadened through free propagation and which therefore can be approximated by a Gaussian function as

$$A(x) \approx \exp(-0.5x^2/w^2), \tag{4}$$

#182813 - $15.00 USD Received 7 Jan 2013; revised 8 Mar 2013; accepted 15 Mar 2013; published 22 Mar 2013

where w denotes the $1/e$ half width of the envelope function. The field profile in the ideal case at the focal plane of the second FPR is consequently given by

$$E_I(u) = \int E(x) e^{i2\pi\zeta ux} dx = c_1 \left[\mathrm{comb}\left(\Lambda\zeta u\right) * \mathrm{sinc}\left(N\Lambda\zeta u\right) * e^{-\frac{(2\pi w\zeta u)^2}{2}} \right] \times e^{-\frac{(2\pi\sigma\zeta u)^2}{2}}, \qquad (5)$$

where c_1 is a constant factor, and $\zeta \equiv n_s \cos\theta_d / f\lambda$ is the transform factor between the x and u coordinates, and where f is the effective focal length of the 2nd FPR determined by the curvature of the output plane of the waveguide array.

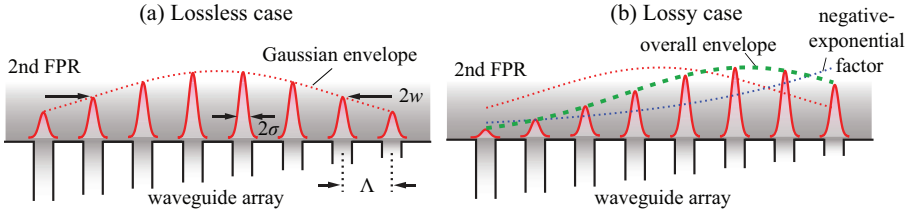

Fig. 2. The envelope function $A(x)$ at the output plane of the waveguide arrays when the waveguides are (a) lossless and (b) with associated loss.

Different teeth of the comb function term in Eq. (5) represent different diffraction orders, which by definition do not overlap with each other. Meanwhile, the spatial width of the waveguide mode σ is also by design much smaller than $N\Lambda$. The value of w in Eq. (5) can be controlled by the size of the first FPR, and typically is comparable to or larger than $N\Lambda$ such that light can be coupled into all waveguides in the array. Hence, in the ideal case in which the loss is negligible, the spot size of the output beam of an AWG is essentially limited by the width of the sinc function in Eq. (5), i.e., by the total number of waveguides in the array, through the following relation

$$\delta u_I = \frac{1}{N\Lambda\zeta} = \frac{f\lambda}{N\Lambda n_s \cos\theta_d}. \qquad (6)$$

Combining Eqs. (2) and (6), one can obtain the following expression for the spectral resolution of an ideal slow-light array-waveguide-grating spectrometer:

$$\delta\omega_I = \delta u_I \frac{d\omega}{du} = \frac{\delta u_I}{f}\frac{d\omega}{d\theta} = \frac{f\lambda}{N\Lambda n_s\cos\theta_d}\frac{n_s n_{\mathrm{eff}}\omega^2\Lambda\cos\theta_d}{2\pi c n_g m f} = \frac{n_{\mathrm{eff}}\omega_0}{N m n_g}, \qquad (7)$$

where $\omega_0 = 2\pi c/\lambda_0$ is the center angular frequency. This expression shows that the spectral resolution of an ideal slow-light AWG is determined by three factors, namely, the total number N of waveguides in the array, the diffraction order m, and the group index n_g of the waveguides. Meanwhile, it can be shown that the free spectral range of a slow-light AWG is given by [11]

$$\mathrm{FSR} = \frac{n_{\mathrm{eff}}\omega_0}{n_g m}. \qquad (8)$$

Thus, the maximum number of resolvable spectral lines of an ideal slow-light AWG is approximately equal to $\mathrm{FSR}/\delta\omega_I = N$, i.e., the number of waveguides in the waveguide array. Note that the footprint of an AWG scales as the number of waveguides multiplied by the average waveguide length, i.e., the footprint scales as $N^2 m\lambda$. One sees from Eq. (7) that by using slow-light waveguides, the footprint of an AWG with a fixed spectral resolution scales as $1/n_g^i$, where $1 \ll i \ll 2$ depending on the choice between N and m.

#182813 - $15.00 USD Received 7 Jan 2013; revised 8 Mar 2013; accepted 15 Mar 2013; published 22 Mar 2013

When the waveguides are lossy, the transmission through waveguides of increasing lengths is no longer equal. The output envelope function is consequently modified as

$$A(x) = \exp\left(-\tfrac{1}{2}x^2/w^2\right)\exp\left[-\tfrac{1}{2}\alpha'(x+N\Lambda/2)\right], \tag{9}$$

where $\alpha' = \alpha\Delta l/\Lambda$ is the effective loss coefficient mapped onto the transverse coordinate x along the input of the 2nd FPR, and where α is the loss coefficient of the waveguide. As illustrated in Fig. 2(b), the extra negative exponential function can cause significant modification of the envelope function $A(x)$ in terms of both the peak position and the effective width. Consequently, the output field profile at the focal plane of the second FPR is given by

$$\begin{aligned} E_L(u) &= \int E(x)e^{i2\pi\zeta ux}dx \\ &= c_2\left[\mathrm{comb}\left(\Lambda\zeta u\right) * \mathrm{sinc}\left(N\Lambda\zeta u\right) * e^{-\frac{(2\pi w\zeta u)^2}{2}} * \frac{e^{i\pi N\Lambda\zeta u}}{u^2+\left(\frac{\alpha'}{2\pi\zeta}\right)^2}\right] \times e^{-\frac{(2\pi\sigma\zeta u)^2}{2}}, \end{aligned} \tag{10}$$

where c_2 is a constant factor. One sees that the spatial profile of the output beam for a lossy AWG is that of an ideal AWG convolved with a Lorentzian function. Thus, the beam spot size is limited not only by the total number of waveguides in the array through the sinc function, but also by the loss coefficient of the waveguides through the Lorentzian function. In the limit in which N is sufficiently large, the minimum spot size becomes fundamentally bounded by the width of the loss-induced Lorentzian function through

$$\delta u_L = \frac{\alpha'}{2\pi\zeta} = \frac{\alpha\Delta l f\lambda}{2\pi\Lambda n_\mathrm{s}\cos\theta_\mathrm{d}}. \tag{11}$$

Combining Eqs. (2) and (11), one can obtain the following expression for the loss-limited spectral resolution for an AWG using lossy slow-light waveguides:

$$\delta\omega_L = \delta u_L\frac{d\omega}{du} = \frac{\delta u_L}{f}\frac{d\omega}{d\theta} = \frac{\alpha\Delta l f\lambda}{2\pi\Lambda n_\mathrm{s}\cos\theta_\mathrm{d}}\frac{n_\mathrm{s}n_\mathrm{eff}\omega^2\Lambda\cos\theta_\mathrm{d}}{2\pi cn_g mf} = \frac{c\alpha}{n_g}. \tag{12}$$

One sees that the minimum spectral resolution for an AWG with lossy slow-light waveguides is always bounded by the velocity of light c times the loss–group-index ratio α/n_g. This result is also consistent with previous studies of other types of interferometric spectrometers [9].

3. Numerical analysis

To better illustrate our analytical predictions, we plot in Fig. 3 the minimum spectral resolution of an AWG as a function of the group index and the loss coefficient, within reported values of the group index ranging from 10 to 200, and the loss coefficient ranging from 15 to 200 dB/cm.

In particular, we pick out three sets of values for n_g and α as typical examples of currently available slow-light photonic crystal waveguides [15, 16]. Point A refers to a typical design of a dispersion engineered W1 flat-band photonic crystal waveguide [17], whose group index and loss coefficient are approximately 30 and 80 dB/cm, respectively. The minimum spectral resolution of an AWG using such a flat-band PhC waveguide is approximately 4 GHz. Note that the fundamental limiting spectral resolution of an AWG using such dispersion-engineered slow-light waveguides is already comparable to or less than that of conventional approaches, whose minimum spectral resolution is currently of the order of 5 GHz [18].

Note that the slow-light bandwidth $\Delta\lambda_\mathrm{sl}$ of such a flat-band slow-light waveguide over which the group index is maintained at 30 within 5% variation is approximately 10 nm [17]. The

#182813 - $15.00 USD Received 7 Jan 2013; revised 8 Mar 2013; accepted 15 Mar 2013; published 22 Mar 2013

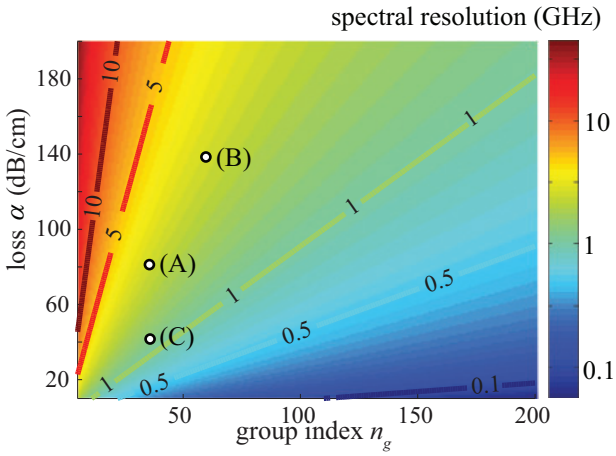

Fig. 3. Minimum achievable spectral resolution of a slow-light AWG defined by Eq. (12) as a function of the group index n_g and loss coefficient α of the waveguides.

working bandwidth of the slow-light AWG spectrometer is then determined by the smaller of $\Delta\lambda_{\mathrm{sl}}$ and its FSR. Note that since the footprint of an AWG scales at least linearly with $1/n_g$, a slow-light AWG using waveguides with $n_g \approx 30$ has a footprint at least 8 times smaller than that of an conventional AWG using conventional waveguides with $n_g \approx 4$. Using dispersion engineered designs, one can also achieve a larger group index, but it is typically associated with larger loss (see point B in Fig. 3) and narrower slow-light bandwidth [16, 17]. While the achievable spectral resolution is almost the same since the ratio of α/n_g does not change significantly, the footprint can be further reduced because of the large value of n_g.

Beside dispersion engineering, loss engineering on PhC waveguide designs has also been recently studied [15, 16, 19]. Using such approaches, one can achieve a group index of 30 with further reduced loss of 40 dB/cm. In such a case, the loss-limited spectral resolution (see point C in Fig. 3) can be further improved to be less than 2 GHz. As the design and fabrication process of PhC slow-light waveguides becomes further refined such that one can achieve group index and loss coefficient with values falling in the right-bottom portion of Fig. 3, one can potentially obtain spectral resolution of sub-GHz.

4. Summary

In summary, we have analytically derived an expression for the limiting spectral resolution of an AWG spectrometer in the presence of loss. We have shown that when the waveguide is lossy, the minimum achievable spectral resolution scales as the loss–group-index ratio of the waveguides used in the AWG. We have also shown that an AWG spectrometer using currently available loss-engineered PhC slow-light waveguides can already achieve spectral resolutions better than those of conventional approaches, with a much reduced footprint. As the design and fabrication of PhC waveguide is further improved with a further reduced loss–group-index ratio, one can potentially achieve spectral resolution of sub-GHz, sufficient for many spectroscopic applications such as chemical and biological substance recognition. Our analysis is applicable for other types of grating-based spectrometers, and it provides guidelines for developing on-chip slow-light spectroscopic devices to meet specific demands on the spectral performance. This project received support from the Defense Threat Reduction Agency-Joint Science and Technology Office for Chemical and Biological Defense (grant no. HDTRA1-10-1-0025).

#182813 - $15.00 USD Received 7 Jan 2013; revised 8 Mar 2013; accepted 15 Mar 2013; published 22 Mar 2013